Enantioselective CD Sensing of Cysteine and Glutathione with Gold Nanorods.

ARTICLE *in* ANALYTICAL CHEMISTRY · DECEMBER 2014

Impact Factor: 5.64 · DOI: 10.1021/ac504017f · Source: PubMed

5 AUTHORS, INCLUDING:

Xinyu Li
Harbin Institute of Technology
10 PUBLICATIONS **289** CITATIONS
SEE PROFILE

Mei Yan
Harbin Institute of Technology
16 PUBLICATIONS **341** CITATIONS
SEE PROFILE

Shaoqin Liu
Harbin Institute of Technology
75 PUBLICATIONS **2,128** CITATIONS
SEE PROFILE

analytical chemistry

Letter

pubs.acs.org/ac

Enantioselective Circular Dichroism Sensing of Cysteine and Glutathione with Gold Nanorods

Fu Zhu,[†,‡] Xinyu Li,[†,‡] Yuchen Li,[†,‡] Mei Yan,*[,†] and Shaoqin Liu*[,†]

[†]Key Laboratory of Microsystems and Microstructures Manufacturing, Ministry of Education, Harbin Institute of Technology, Harbin, 150080, China

[‡]School of Life Science and Technology, Harbin Institute of Technology, Harbin, 150080, China

Supporting Information

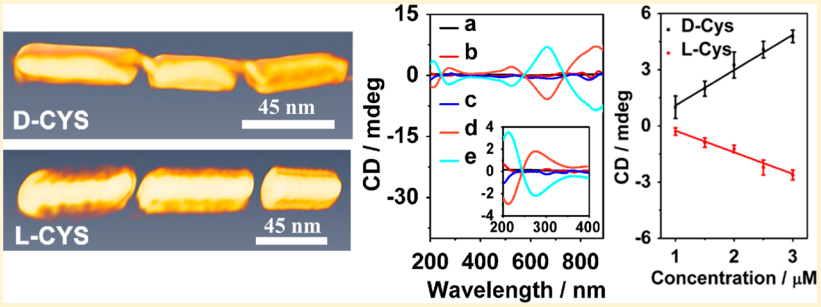

ABSTRACT: Enantioselective analysis of biological thiols, including cysteine (Cys) and glutathione (GSH), is extremely important because of their unique role in bioentities. Here we demonstrated that the end-to-end assemblies of plasmonic gold nanorods with chiral Cys or GSH can be used as a distinctive chiroptical sensor for reliable determination of the absolute configuration of Cys and GSH at the visible light region. The end-to-end assemblies of Au nanorods induced by Cys or GSH exhibit strong circular dichroism (CD) signals in the region of 500−850 nm, which is attributed to chiral current inside Au nanorods induced by the mixed biothiols. The CD intensity of the assemblies shows good linearity with the amount of Cys and GSH. The limit of detection for Cys and GSH using end-to-end assemblies is at micromolar concentrations. In addition, the sensing system exhibits good selectively toward Cys and GSH in the presence of other amino acids.

Chiral species play an essential role in medical and biochemical systems, and thus enantioselective analysis of chiral molecules has become a central aspect in chemical, biological, medical research, and pharmaceutical industry.[1] Among those, biological thiols such as glutathione (GSH) and cysteine (Cys) have gained much attention in recent years due to their vital biological functions in neuronal tissues, brain, metabolism, detoxification, and protein synthesis.[2−7] As an example, previous studies have demonstrated the importance of the chiral configuration of Cys in the nervous system. Low levels of L-Cys normally functions as a neuromodulator or a neuroprotective antioxidant in neuronal activity,[8] while high levels of L-Cys may lead to damage and a neurotoxic effect that may cause following neuronal trauma such as brain ischemia.[9] In contrast, D-Cys does not cause excitotoxic damage to the brain[10] and protects cerebellar neurons more efficiently from oxidative stress induced by hydrogen peroxide.[11] Various analytical methods targeted to GSH and Cys recognition have been reported, such as high-performance liquid chromatography,[12] gas chromatography/mass spectrometry,[13] electrochemistry, [14] and the molecularly imprinted technique.[15] Although remarkable progress has been made in the field of instrumental analytical methods, few cases have been reported on development of time- and cost-effective sensing techniques with potential for high-throughput stereoselective analysis of GSH and Cys. In this regard, chiroptical methods have been proven to be quite versatile. The key of chiroptical methods is to find a suitable chiral receptor that could change its optical activity significantly upon enantioselective binding to a chiral substrate. A wide range of fluorescence probes have been reported for analysis of the absolute configuration and accurate quantification of amino acids.[16−21] In addition to fluorescent probes, many examples of chirality sensing of amino acid with circular dichroism (CD) probes have also been proposed.[22−34] In this method, the CD probes are usually metal complexes or the configurationally flexible biphenyl chromophores, which are capable of binding the N- or O-group of amino acids through noncovalent interactions, such as coordination force[35−38] or hydrogen bonding.[23,28,31,33,39] The association of amino acids with these probes results in an induced CD response. It is worth mentioning that although this approach is able to achieve enantioselective discrimination of the amino acids, most CD probes could not selectively differentiate Cys or GSH from other 19 types of amino acids. Therefore, finding a specific CD

Received: October 27, 2014
Accepted: December 6, 2014
Published: December 6, 2014

   dx.doi.org/10.1021/ac504017f | *Anal. Chem.* 2015, 87, 357−361

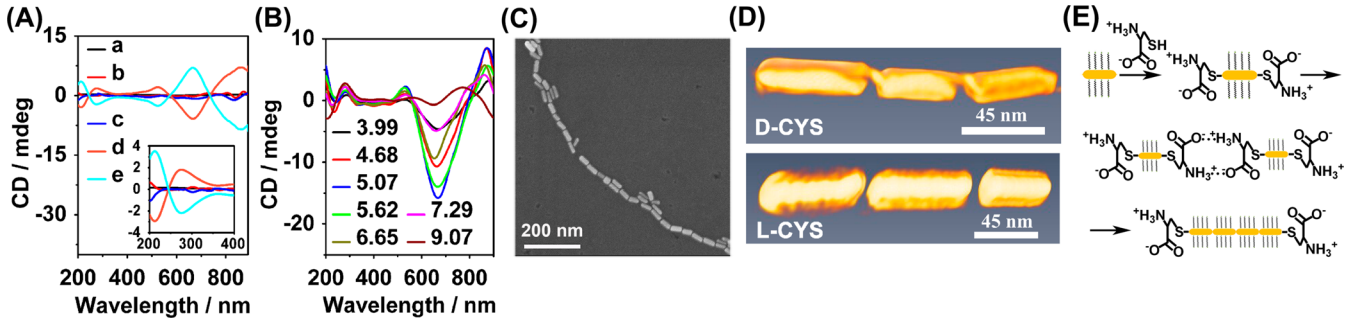

Figure 1. (A) CD spectra of Au nanorod alone (a), L-Cys (b) or D-Cys alone (c), and mixture of Au nanorods and L-Cys (d) or D-Cys (e). The concentration of Cys and Au nanorods is set to 10 μM and 0.37 nM, respectively. (B) CD spectra of the mixture of L-Cys and Au nanorods at various pH. (C) SEM image of Au nanorods after addition of L-Cys at pH 5.07. (D) Cryo TEM tomography images for Cys-induced end-to-end assembly of Au nanorod. (E) Cys-induced end-to-end assembly of Au nanorods.

probe, which is capable of fast and sensitive detection of the chirality of Cys and GSH, is becoming highly desirable.[40]

Gold (Au) nanorods exhibit rich surface-plasmon-resonance (SPR)-derived properties, which have made them particularly useful for optical sensing, e.g., UV−vis absorption measurement or surface-enhanced Raman scattering detection.[41−44] Recently, the emerging chiroptical properties of Au nanorods originating from the adsorbed chiral organic molecules or their assemblies induced by chiral templates (for example, DNA and peptide) are intriguing,[45−47] which is offering the new opportunity for analytical applications.[46] In this study, we decided to explore the potential of Au nanorods as amplifiers of molecular chirality of Cys and GSH. Au nanorods were synthesized by adopting a seed-mediated growth method.[47] The characteristic transverse SPR (TSPR) and longitudinal SPR (LSPR) absorption peaks of as-prepared Au NRs are 515 and 710 nm, respectively (Figure S1A in Supporting Information). The corresponding extinction values at these two SPR peaks are 0.7 and 2.2, respectively, suggesting a high yield of Au nanorods. Transmission electron microscopy (TEM) imaging further demonstrates that the Au nanorods possess a uniform diameter and length of 13.1 and 40.8 nm, respectively, with an aspect ratio of 3.1 (Figure S1B in the Supporting Information).

We first performed a CD investigation on pure Au nanorods or Cys molecules (Figure 1). No CD signal is observed for pure Au nanorods in the absence of a chiral guest, in agreement with the fact that Au nanorods are nonchiral (curve a in Figure 1A). Meanwhile, no CD response above 300 nm is discerned for the enantiomers of Cys alone even at elevated concentrations (curves b and c in Figure 1A). Thus, any signals recognized at the wavelength of above 300 nm should be attributed to the formation of Au nanorods and chiral Cys complexes. Subsequent addition of either enantiomer of Cys to Au nanorods could give evident chiroptical signatures in CD spectra (curves d and e in Figure 1A). The CD signals appear immediately after the samples are mixed, and all measurements have been taken within 5 min. A small CD signal in the UV region, located at ∼220 nm, should be assigned to chiral optical absorption of Cys. Besides, the much stronger CD response appears at the wavelength of 500−850 nm, corresponding to TSPR and LSPR absorption of Au nanorods, respectively. These new CD responses in the visible light region are believed to be caused by chiral current inside Au nanorods induced by the mixed Cys,[48] which are thus called as plasmonic CD responses.[49] A closer look at the sign of the maximum CD amplitudes reveals that enantiometric substrates yield the products with opposite Cotton effects. A positive CD maximum is observed for Cys with an *S* configuration while the opposite CD response was observed for *R* Cys. Accordingly, the induced chirality of Au nanorods is directly correlated to the central chirality of Cys. The optical anisotropy factor (*g*-factor) for the longitude LSPR wavelength was -0.28×10^{-4} in the presence of 10 μM Cys. Furthermore, our experimental results demonstrate that such plasmonic CD responses in the visible light region are sensitive to the pH value of solution. Figure 1B summarizes the CD spectra of the mixture of L-Cys and Au nanorods at various pH. A strong negative maximum at about 670 nm is seen at all pH tested. The maximum CD signal appears at pH 5.07, and both increasing and decreasing pH of mixture result in the decrease in CD response.

The CD spectra of the mixture of Au nanorods and Cys clearly demonstrate occurrence of a chirality transfer from L- or D-Cys to the Au nanorods, which is most efficient at the isoelectric point of Cys (pH 5.02). The chirality transfer phenomenon could be assigned to the induced assembly of Au nanorods by Cys, which is covalently bound to the ends of Au nanorods and induces the assembly of Au nanorods through electrostatic interaction between Au nanorods. This end-to-end assembly is confirmed by UV−vis spectra and scanning electron microscopy (SEM) imaging. The addition of Cys to Au nanorods resulted in the dramatic decrease in the intensity of the LSPR absorption band, with a concomitant formation of a new red-shifted band at 800 nm from the coupling of the plasmon absorption of Au nanorods through self-assembly (Figure S2A,B in the Supporting Information). SEM studies show that the Au nanorods before addition of Cys are randomly distributed (Figure S3 in the Supporting Information), whereas linear-chain morphology of Cys-bound rods is achieved (Figure 1C). The three-dimensional images of the assemblies obtained with cryo transmission electron microscopy (TEM) tomography showed both end-to-end Au NR assemblies induced by either L-Cys (bottom image) or D-Cys (up image) display a linear 1D structure (Figure 1D and movie in the Supporting Information). The assumption is in agreement with the observed maximum CD response at pH 5.07 in Figure 1B. The isoelectric point of Cys is reported as 5.02, while the pK_a values of the carboxyl and amino groups of Cys are 2.0 and 10.3, respectively. At pH 5.07, two-point electrostatic interactions between the protonated amine and the deprotonated carboxylate group facilitate an end-to-end self-assembly (Figure 1E), resulting in an enhanced CD intensity.

To evaluate the practical use of Au nanorods for plasmonic CD detection of chiral Cys, we measured the CD readout of Au nanorods with different concentrations of Cys. To 5.4 mL of

dx.doi.org/10.1021/ac504017f | *Anal. Chem.* 2015, 87, 357−361

0.37 nM Au nanorod, a different concentration of Cys was added and allowed to stir for 1 min, followed by CD measurements. Impressively, a linear relationship is found between the CD amplitude of Au nanorods and the concentration of Cys in the range of 1−3 μM, as shown in Figure 2. The linear regression equation is CD = 0.8988 − 1.1531$C_{L\text{-}Cys}$ (R^2 = 0.97, n = 5) for L-Cys and CD = −0.7931 + 1.8862$C_{D\text{-}Cys}$ (R^2 = 0.99, n = 5) for D-Cys, respectively. The calculated detection limit was found to be 1.40 for L-Cys and 0.80 μM (3σ/s, n = 5) for D-Cys based on CD intensity at 670 nm, respectively.

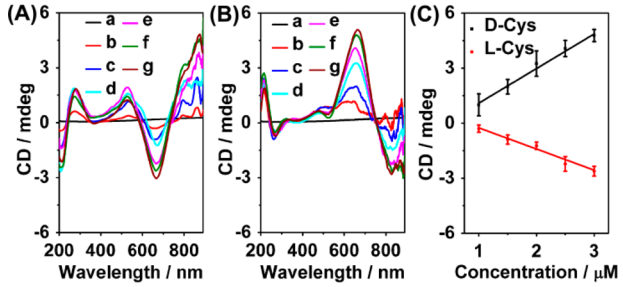

Figure 2. CD spectral changes of Au nanorods upon addition of L-Cys (A) and D-Cys (B). The concentration of L-Cys and D-Cys is as following: (a) 0, (b) 1, (c) 1.5, (d) 2.0, (e) 2.5, (e) 3.0, and (f) 5 μM. (C) The linear relationship between CD signal at 670 nm and the added concentration of D-Cys or L-Cys.

We further investigated the selectivity of Au nanorods by identifying other amino acids. Figure S4 in the Supporting Information summarizes the structures of 19 types of the most common amino acids besides Cys, which have both L- and D-forms. Enantiomers (100 μM) of different amino acids were added to 3 mL of 0.37 nM Au nanorods. Compared with Cys, no considerable CD response in the light region above 300 nm are observed for these 19 types of amino acids even when the concentration of amino acids tested is up to 100 μM (Figure 3A). This result indicates that Au nanorods have much better specificity to Cys. Importantly, adding 10 times of other amino acids to the Au nanorods/Cys system only causes a slight decrease in the CD signals of the system (Figure 3B), implying

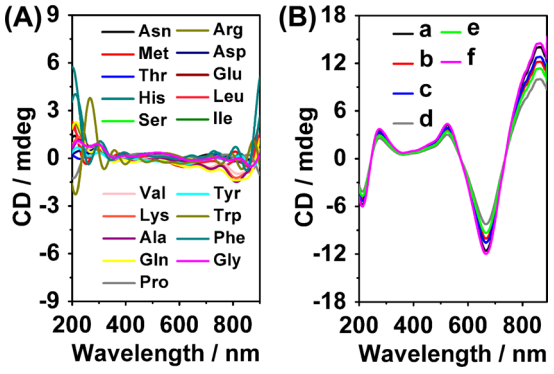

Figure 3. (A) CD response of Au nanorods to the other 19 types of amino acids in the L form besides Cys. The concentration of amino acids and Au nanorods are 100 μM and 0.37 nM, respectively. (B) CD spectra of the Au nanorods/L-Cys system (a) in the presence of Asn (b), Ile (c), Lys (d), Ala (e), Gln (f). The concentration of Cys, other amino acids, and Au nanorods are 10 μM, 100 μM, and 0.23 nM, respectively.

that the presence of other amino acids would not interfere with the enantioselective recognition of Cys. Subsequently, we evaluated the selectivity of Au nanorods toward other thiol-containing species, including 2-sulfanylsuccinic acid. Almost no CD signal was observed (Figure S5 in the Supporting Information). This is consistent with the fact that 2-sulfanylsuccinic acid has only two carboxylic groups and no amine group. Therefore, electrostatic repulsion between Au nanorods, which are covalently bonded with 2-sulfanylsuccinic acid, impeded the end-to-end assembly.

The chiroptical response of Au nanorods after addition of tripeptide GSH is also investigated. We found that Au nanorods were also suitable for enantioselective recognition of GSH. The CD sensing of GSH gives a strong Cotton effect corresponding to the SPR bands of Au nanorods in the region of 500−800 nm (Figure 4A), and the CD amplitude at 670 nm increases with

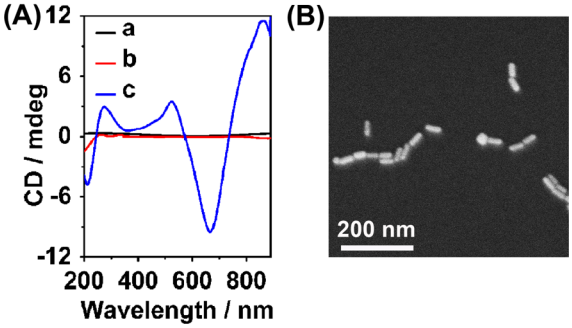

Figure 4. (A) CD spectra of Au nanorod alone (a), L- GSH (b), and the mixture of Au nanorods and L-GSH (c). (B) SEM image of Au nanorods after addition of GSH.

increasing the amount of GSH (Figure S6 in the Supporting Information). The linear calibration curve is obtained within 1−5 μM for L-GSH, and a linear regression equation is CD = 2.0078 − 2.1880$C_{L\text{-}GSH}$ (R^2 = 0.98, n = 5), achieving a detection limit of 1.93 μM (3σ/s, n = 5) and a precision of 6.1% RSD (5 μM, n = 5). The appearance of CD signal can also be attributed to the end-to-end assembly induced by GSH binding to the ends of Au nanorods.[50] However, comparing the CD response of the Au nanorods/Cys system with Au nanorods/GSH system (Figure S7 in the Supporting Information), it can be found that the CD signals of the Au nanorods in the presence of Cys appear immediately and gradually decrease upon exposure to air (Figure S7A in the Supporting Information), while in the case of GSH CD signals appear after mixing for 10 min and achieve the maximum CD amplitude at ∼1 h (Figure S7B in the Supporting Information). The slower response observed for the Au nanorods/GSH system is also confirmed by SEM observation. Figure 4B shows a representative SEM image of Au nanorods in the presence of 10 μM GSH for 1 h. The Au nanorods are linked together at their ends, but the number of end-to-end assembled nanorods is fewer than that in the presence of Cys. The difference in CD response time probably originates from the larger size of GSH that affects its binding to the ends of Au nanorods.[51] On the basis of different response times of Au nanorods to Cys and GSH, we can assume that the presence of GSH does not probably interfere with determination of Cys. Indeed, addition of 10 μM GSH to the Au nanorods/Cys system does not immediately increase the CD amplitude (Figure S8 in the Supporting Information).

dx.doi.org/10.1021/ac504017f | Anal. Chem. 2015, 87, 357−361

In conclusion, we demonstrate that the end-to-end assembly of Au nanorods can be used for chirality sensing of Cys. This novel enantioselective sensing strategy is based on the end-to-end assemblies of Au nanorods and chiral Cys. The collective optical activity in the assemblies can easily be measured by CD spectroscopy, and the sign and the amplitude of the Cotton effect are explored to correlate with the absolute configuration and concentration of Cys. Compared to the reported CD probes, the observed Cotton effects occur in the visible light region with longer wavelengths (between 500 and 800 nm), which effectively eliminates interference from CD active analytes as well as improves the detection reliability (the visible light detector is more sensitive than the UV detector). Moreover, the CD spectra of Au nanorods remain almost unaffected upon addition of various amino acids other than Cys and GSH. It is highly expected that such CD responses based on assemblies of noble metal nanoparticles and chiral biomolecules will provide a facile and versatile platform for enantioselective analysis of important species related to biological processes.

■ ASSOCIATED CONTENT

Supporting Information

Experimental section and other characterization data as noted in the text. This material is available free of charge via the Internet at http://pubs.acs.org.

■ AUTHOR INFORMATION

Corresponding Authors

*E-mail: yanmei@hit.edu.cn.

*E-mail: shaoqinliu@hit.edu.cn.

Notes

The authors declare no competing financial interest.

■ ACKNOWLEDGMENTS

This work was kindly supported by the National Natural Science Foundation of China (Grant Nos. 51372054 and 21161120325) and Outstanding Young Funding of Heilongjiang Province.

■ REFERENCES

(1) Pu, L. *Chem. Rev.* **2004**, *104*, 1687−1716.

(2) Weerapana, E.; Wang, C.; Simon, G. M.; Richter, F.; Khare, S.; Dillon, M. B. D.; Bachovchin, D. A.; Mowen, K.; Baker, D.; Cravatt, B. F. *Nature* **2010**, *468*, 790−795.

(3) Janáky, R.; Varga, V.; Hermann, A.; Saransaari, P.; Oja, S. S. *Neurochem. Res.* **2000**, *25*, 1397−1405.

(4) Droöge, W.; Holm, E. *FASEB J.* **1997**, *11*, 1077−1089.

(5) Wood, Z. A.; Schroder, E.; Harris, J. R.; Poole, L. B. *Trends Biochem. Sci.* **2003**, *28*, 32−40.

(6) Fiser, B.; Szőri, M.; Jójárt, B.; Izsák, R.; Csizmadia, I. G.; Viskolcz, B. *J. Phys. Chem. B* **2011**, *115*, 11269−11277.

(7) Axelsson, K.; Mannervik, B. *FEBS Lett.* **1983**, *152*, 114−118.

(8) Brosnan, J. T.; Brosnan, M. E. *J. Nutr.* **2006**, *136*, 1636S−1640S.

(9) Slivka, A.; Cohen, G. *Brain Res.* **1993**, *608*, 33−37.

(10) Misra, C. H. *Neurochem. Res.* **1989**, *14*, 253−257.

(11) Shibuya, N.; Koike, S.; Tanaka, M.; Ishigami-Yuasa, M.; Kimura, Y.; Ogasawara, Y.; Fukui, K.; Nagahara, N.; Kimura, H. *Nat. Commun.* **2013**, *4*, 1366.

(12) Qin, L.; He, X. W.; Li, W. Y.; Zhang, Y. K. *J. Chromatogr., A* **2008**, *1187*, 94−102.

(13) Kaspar, H.; Dettmer, K.; Gronwald, W.; Oefner, P. J. *J. Chromatogr., B* **2008**, *870*, 222−232.

(14) Fu, Y. Z.; Han, Q.; Chen, Q.; Wang, Y. H.; Zhou, J.; Zhang, Q. *Chem. Commun.* **2012**, *48*, 2322−2324.

(15) (a) Zhang, Y. X.; Zhao, P. Y.; Yu, L. P. *Sens. Actuators, B* **2013**, *181*, 850−857. (b) Cai, X. Q.; Li, J. H.; Zhang, Z.; Wang, G.; Song, X. L.; You, J. M.; Chen, L. X. *Talanta* **2014**, *120*, 297−303.

(16) Niu, L. Y.; Guan, Y. S.; Chen, Y. Z.; Wu, L. Z.; Tung, C. H.; Yang, Q. Z. *J. Am. Chem. Soc.* **2012**, *134*, 18928−18931.

(17) Liu, J.; Sun, Y. Q.; Huo, Y. Y.; Zhang, H. X.; Wang, L. F.; Zhang, P.; Song, D.; Shi, Y. W.; Guo, W. *J. Am. Chem. Soc.* **2014**, *136*, 574−577.

(18) He, X.; Cui, X.; Li, M. S.; Lin, L. L.; Liu, X. H.; Feng, X. M. *Tetrahedron Lett.* **2009**, *50*, 5853−5856.

(19) Lin, J.; Li, Z. B.; Zhang, H. C.; Pu, L. *Tetrahedron Lett.* **2004**, *45*, 103−106.

(20) Corradini, R.; Paganuzzi, C.; Marchelli, R.; Pagliari, S.; Sforza, S.; Dossena, A.; Galaverna, G.; Duchateau, A. *J. Mater. Chem.* **2005**, *15*, 2741−2746.

(21) Zhang, X. L.; Zheng, C.; Guo, S. S.; Yang, H. H.; Chen, G. N. *Anal. Chem.* **2014**, *86*, 3426−3434.

(22) Corradini, R.; Dossena, A.; Impellizzeri, G.; Maccarrone, G.; Marchelli, R.; Rizzarelli, E.; Sartor, G.; Vecchio, G. *J. Am. Chem. Soc.* **1994**, *116*, 10267−10274.

(23) Holmes, A. E.; Zahn, S.; Canary, J. W. *Chirality* **2002**, *14*, 471−477.

(24) Ogoshi, H.; Mizutani, T. *Acc. Chem. Res.* **1998**, *31*, 81−89.

(25) Huang, X.; Fujioka, N.; Pescitelli, G.; Koehn, F. E.; Williamson, R. T.; Nakanishi, K.; Berova, N. *J. Am. Chem. Soc.* **2002**, *124*, 10320−10335.

(26) Balaz, M.; De Napoli, M.; Holmes, A. E.; Mammana, A.; Nakanishi, K.; Berova, N.; Purrello, R. *Angew. Chem., Int. Ed.* **2005**, *44*, 4006−4009.

(27) Superchi, S.; Bisaccia, R.; Casarini, D.; Laurita, A.; Rosini, C. *J. Am. Chem. Soc.* **2006**, *128*, 6893−6902.

(28) Bentley, K. W.; Nam, Y. G.; Murphy, J. M.; Wolf, C. *J. Am. Chem. Soc.* **2013**, *135*, 18052−18055.

(29) You, L.; Berman, J. S.; Anslyn, E. V. *Nat. Chem.* **2011**, *3*, 943−948.

(30) You, L.; Pescitelli, G.; Anslyn, E. V.; Di Bari, L. *J. Am. Chem. Soc.* **2012**, *134*, 7117−7125.

(31) Dutot, L.; Wright, K.; Gaucher, A.; Wakselman, M.; Mazaleyrat, J. P.; De Zotti, M.; Peggion, C.; Formaggio, F.; Toniolo, C. *J. Am. Chem. Soc.* **2008**, *130*, 5986−5992.

(32) Bentley, K. W.; Wolf, C. *J. Am. Chem. Soc.* **2013**, *135*, 12200−12203.

(33) Kim, H.; So, S. M.; Yen, C. P.-H.; Vinhato, E.; Lough, A. J.; Hong, J.-I.; Kim, H. J.; Chin, J. *Angew. Chem., Int. Ed.* **2008**, *47*, 8657−8660.

(34) Wolf, C.; Bentley, K. W. *Chem. Soc. Rev.* **2013**, *42*, 5408−5424.

(35) Folmer-Andersen, J. F.; Lynch, V. M.; Anslyn, E. V. *Chem.—Eur. J.* **2005**, *11*, 5319−5326.

(36) Joyce, L. A.; Canary, J. W.; Anslyn, E. V. *Chem.—Eur. J.* **2012**, *18*, 8064−8069.

(37) Buryak, A.; Severin, K. *J. Am. Chem. Soc.* **2005**, *127*, 3700−3701.

(38) Joyce, L. A.; Maynor, M. S.; Dragna, J. M.; da Cruz, G. M.; Lynch, V. M.; Canary, J. W.; Anslyn, E. V. *J. Am. Chem. Soc.* **2011**, *133*, 13746−13752.

(39) Mazaleyrat, J. P.; Wright, K.; Gaucher, A.; Toulemonde, N.; Wakselman, M.; Oancea, S.; Peggion, C.; Formaggio, F.; Setnicka, V.; Keiderling, T. A.; Toniolo, C. *J. Am. Chem. Soc.* **2004**, *126*, 12874−12879.

(40) Shibuya, N.; Kimura, H. *Front. Endocrinol.* **2013**, *4*, 87.

(41) Xu, L.; Kuang, H.; Wang, L.; Xu, C. *J. Mater. Chem.* **2011**, *21*, 16759−16782.

(42) Wang, L.; Zhu, Y.; Xu, L.; Chen, W.; Kuang, H.; Liu, L.; Agarwal, A.; Xu, C.; Kotov, N. A. *Angew. Chem., Int. Ed.* **2010**, *49*, 5472−5475.

(43) Sudeep, P. K.; Joseph, S. T. S.; Thomas, K. G. *J. Am. Chem. Soc.* **2005**, *127*, 6516−6517.

(44) Rex, M.; Hemandez, F. E.; Campiglia, A. D. *Anal. Chem.* **2006**, *78*, 445−451.
(45) (a) Ma, W.; Kuang, H.; Wang, L. B.; Xu, C. L.; Chang, W. S.; Zhang, H. N.; Zhu, Y. Y.; Zhao, Y.; Liu, L. Q.; Xu, C. L.; Link, S.; Kotov, N. A. *Sci. Rep.* **2013**, *3*, 1934. (b) Hao, C. L.; Xu, L. G.; Ma, W.; Wang, L. B.; Kuang, H.; Xu, C. L. *Small* **2014**, *10*, 1805−1812.
(46) (a) Ma, W.; Kuang, H.; Xu, L.; Ding, L.; Xu, C.; Wang, L.; Kotov, N. A. *Nat. Commun.* **2013**, *4*, 2689. (b) Zhu, Y. Y.; Xu, L. G.; Ma, W.; Xu, Z.; Kuang, H.; Wang, L. B.; Xu, C. L. *Chem. Commun.* **2012**, *48*, 11889−11891.
(47) Nikoobakht, B.; El-Sayed, M. A. *Chem. Mater.* **2003**, *15*, 1957−1962.
(48) (a) Zhu, Z. N.; Liu, W. J.; Li, Z. T.; Han, B.; Zhou, Y. L.; Gao, Y.; Tang, Z. Y. *ACS Nano* **2012**, *6*, 2326−2332. (b) Li, Z. T.; Zhu, Z. N.; Liu, W. J.; Zhou, Y. L.; Han, B.; Gao, Y.; Tang, Z. Y. *J. Am. Chem. Soc.* **2012**, *134*, 3322−3325.
(49) (a) Fan, Z.; Govorov, A. O. *Nano Lett.* **2010**, *10*, 2580−2587. (b) Auguie, B.; Alonso-Gomez, J. L.; Guerrero-Martinez, A.; Liz-Marzan, L. M. *J. Phys. Chem. Lett.* **2011**, *2*, 846−851.
(50) (a) Thomas, K. G.; Barazzouk, S.; Ipe, B. I.; Joseph, S. T. S.; Kamat, P. V. *J. Phys. Chem. B* **2004**, *108*, 13066−13068. (b) Sudeep, P. K.; Joseph, S. T. S.; Thomas, K. G. *J. Am. Chem. Soc.* **2005**, *127*, 6516−6517. (c) Zhang, S. Z.; Kou, X. S.; Yang, Z.; Shi, Q. H.; Stucky, G. D.; Sun, L. D.; Wang, J. F.; Yan, C. H. *Chem. Commun.* **2007**, 1816−1818.
(51) Sun, Z. H.; Ni, W. H.; Yang, Z.; Kou, X. S.; Li, L.; Wang, J. F. *Small* **2008**, *4*, 1287−1292.